Report: Compton scattering

Daniel Schury
Daniel.Schury@physik.uni-giessen.de

Benjamin Vollmann
Benjamin.Vollmann@physik.uni-giessen.de

22nd of March, 2011

Supervisor
Yutie Liang

Contents

1 Assignment of tasks

Compton scattering describes the process, in which a photon hits a quasi-free electron and scatters. In this experiment we use a plasctic szintillator as a scattering target and a NaI szintillator as a detector. The photon sources are radioactive caesium and sodium. The goal of the experiment is to measure the Compton Wavelength of backscattered photons, the connection of scattered photon energy and the scattering angle and as a result to determine the electron mass as well as to compare between the calculated cross section and the measured cross section at different angles.

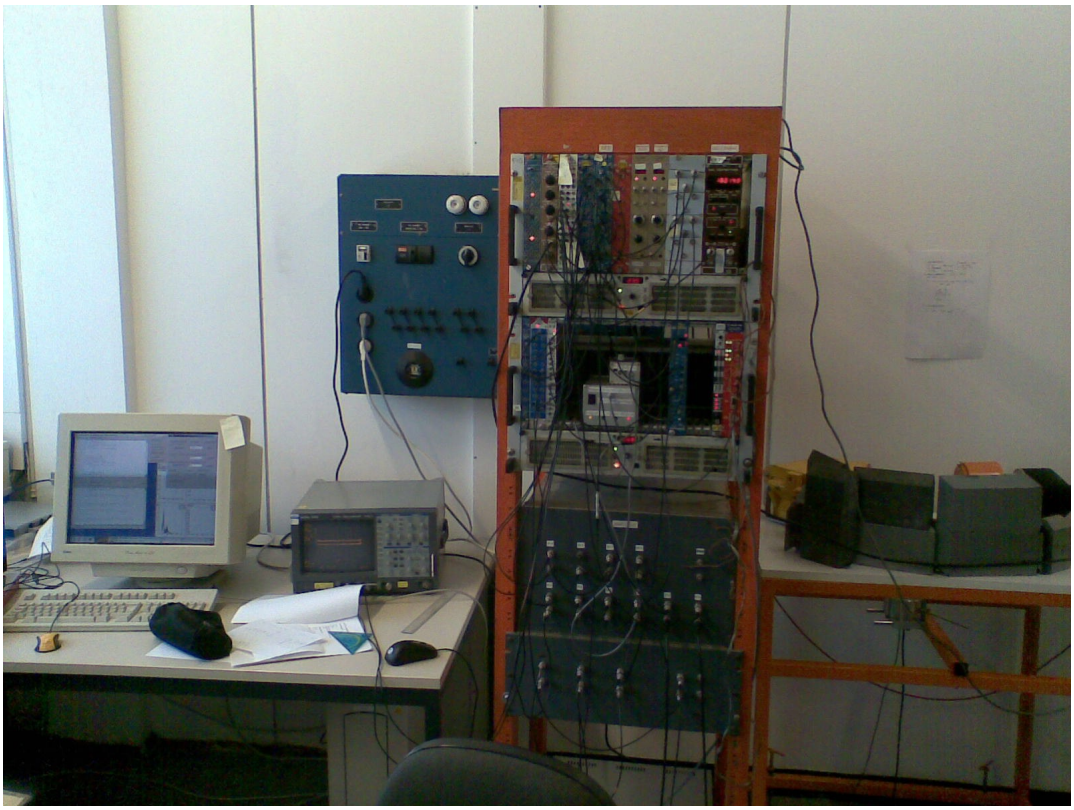

Figure 1.1: Experimental setup

2 Fundamentals

2.1 Sorts of nuclear radiation

Nuclear radiation mainly consists of three different types of radiation: α-, β- and γ-rays. α-rays are nothing more than a two times positive charged helium nucleus. Their energy distribution is a line spectrum and their penetration is quite short. β-rays are electrons/positrons with a continuous energy distribution and a much deeper penetration than α-rays. Last but not least γ-rays consist of photons with an energy of 250 keV up to 10 MeV and more. Because we only use γ-rays in this experiment, we will only talk about them in detail.

2.2 γ-rays

γ-rays are electromagnetic waves with a photon energy between 250 keV and more than 10 MeV. They originate from the interaction of the nucleus with electromagnetic fields. Almost all radioactive elements decay under γ-ray-emission. The nucleus often stays after the decay of α- or β-radiation in an excited state. From there he calms down to its initial state or to a state of a lower energy level while emitting the spare energy as a photon.

$$ {}^{A}_{Z}X^{**} \rightarrow {}^{A}_{Z}X^{*} + \gamma $$

For this reason the energy distribution of γ-rays is discrete, because the distribution of the different energy states is not continuous but discrete, too.

2.2.1 Term scheme of ^{137}Cs and ^{22}Na

Our γ-ray sources are ^{137}Cs and ^{22}Na, at which ^{22}Na is just used to gauge the szintillation detector. Both Term schemes are showed in figure 2.1.
^{137}Cs decays with a probability of 95% through a β^{-}-decay into a stimulated state of ^{137}Ba, from which it relaxes to a stable state of ^{137}Ba by emitting γ-rays of 662 keV. With a small probability of 5 % ^{137}Cs decays direcly into the stable state of ^{137}Ba.
^{22}Na decays through a β^{+}-decay into a stimulated state of ^{22}Ne, from which it relaxes to a stable state of ^{22}Ne by emitting γ-rays of 1,275 MeV. Beside the 1,275 MeV peak you will also find a peak at 511 keV, wich is a result of the β^{+}-decay: The produced positron anhillates with the electron by emitting two gamma-rays of their rest masses.

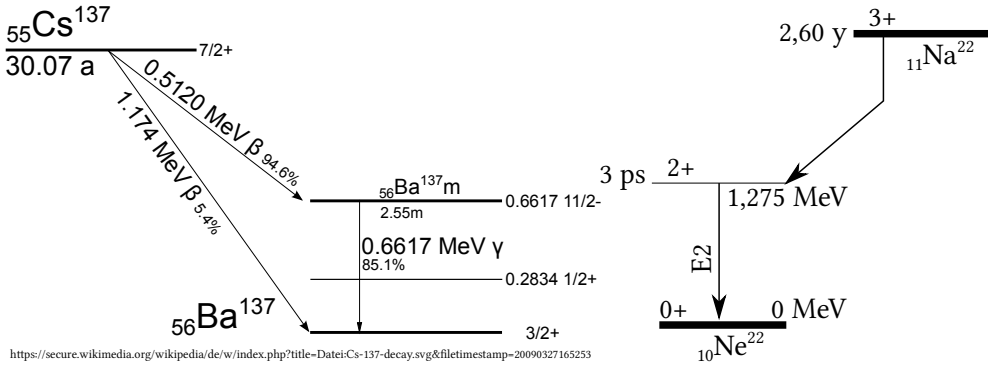

(a) Caesium (b) Sodium

Figure 2.1: Term scheme of ^{137}Cs and ^{22}Na

2.3 Interactions betweeen γ-rays and matter

In general we have three possible interactions between γ-rays and matter: The photoelectric effect, compton scattering and pair production. Figure 2.2 shows at which energy scale which phenomena is dominant.

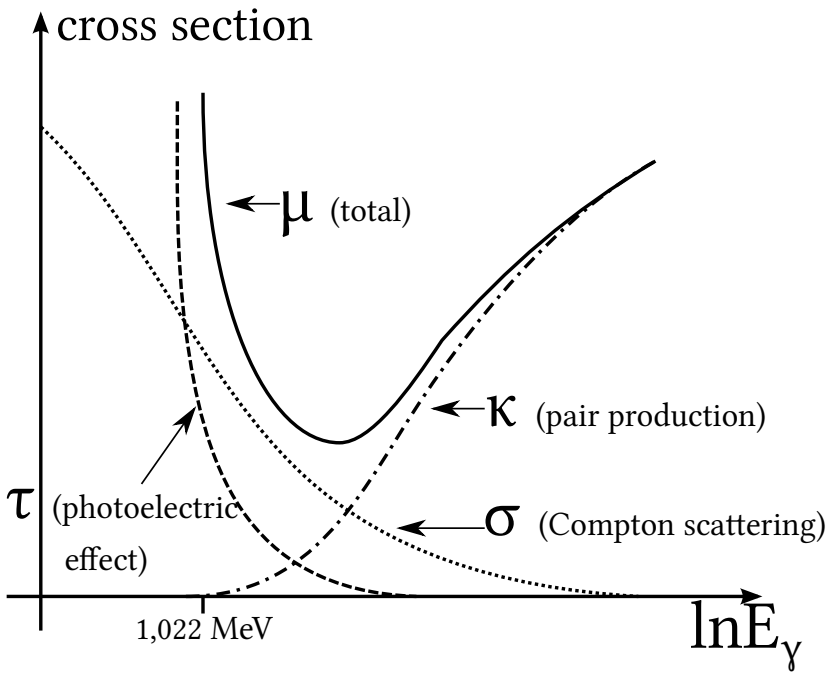

Figure 2.2: Total cross section $\mu = \tau + \sigma + \kappa$

2.3.1 The Photoelectric effect

The photoelectric effect dominates when low-energy photons, with an energy from a few electronvolts up to low numbers of keV, interact with matter. In the photoelectric effect the whole energy of the photons is absorbed by the matter. As a consequence of the absorbtion electrons get kicked off the electron shell. The kinetic energy of the electrons is given by the energy of the incoming photon subtracted by the energy that is needed to set the electron free:

$$E_{kin} = h\nu - W$$

2.3.2 Pair production

Pair production can take place in case of high energies. If you have an amount of energy that is at least equivalent to the double of the rest mass of an electron (511 keV) it is possible to produce an electron positron pair. The production must take place in the close enviroment of a nucleus, otherwise it is not possible to fulfill the conservation of momentum and energy.

2.3.3 Compton scattering

Compton scattering is the dominating phenomena in the mid-energy sector. It describes the scattering of a photon at a nearly disengaged electron. In this case nearly disengaged means, that the bond energy of the electron is small in comparison to the energy of the incoming photon. The phenomena can be solved through a conventional ansatz describing a collision between two bodies. The incoming photon has the energy $E_\gamma = h\nu$ and the momentum $p_\gamma = \frac{h\nu}{c}$, the static electron the energy $E_e = m_e c^2 = 511keV$ and the momentum $p_e = 0$. After the collision the at an angle of *vartheta* scattered photon has the energy $E'_\gamma = h\nu'$ and the momentum $p'_\gamma = \frac{h\nu'}{c}$. The electron gains kinetic energy by the collision whereby it achieves the energy $E'_e = \sqrt{m_e^2 c^4 + p_e'^2 c^2}$ as well as the momentum p'_e. The principle of linear momentum

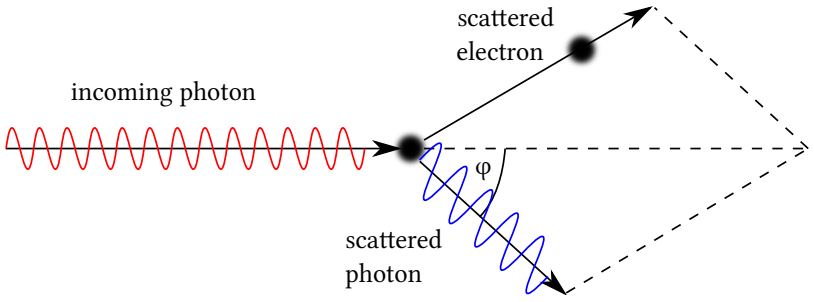

Figure 2.3: Compton scattering

provides

$$\vec{p}_\nu = \vec{p}'_\nu + \vec{p}_e \text{ or rather } \vec{p}_\nu - \vec{p}'_\nu = \vec{p}_e \tag{2.1}$$

If you square this equation you get:

$$p_e'^2 = p_\nu^2 + p_\nu'^2 - 2p_\nu p_\nu' \cdot \cos\vartheta \tag{2.2}$$

From the conservation of energy you get:

$$E_\gamma + E_e = E_\gamma' + E_e' \text{ or rather } h\nu + m_e c^2 = h\nu' + \sqrt{p_e'^2 c^2 + m_e^2 c^4} \tag{2.3}$$

Or:

$$p_e'^2 = \left(\frac{h\nu}{c}\right)^2 + \left(\frac{h\nu'}{c}\right)^2 - 2\frac{h\nu}{c}\frac{h\nu'}{c} + \frac{2m_e c^2}{c^2}(h\nu - h\nu') \tag{2.4}$$

You can now equalize 2.4 and 2.2 and after some additional transformations you get the energy of the scattered photon:

$$h\nu' = \frac{h\nu}{1 + \frac{h\nu}{m_e c^2}(1 - \cos\vartheta)} \tag{2.5}$$

For the inverse energy shift you find

$$\Delta\frac{1}{E} = \frac{1}{h\nu'} - \frac{1}{h\nu} = \frac{1}{m_e c^2}(1 - \cos\vartheta) \tag{2.6}$$

or rather for the modificated wavelength of the scattered photon with $\lambda = \frac{c}{\nu}$

$$\lambda' = \lambda + \frac{h}{m_0 c}(1 - \cos\vartheta) \tag{2.7}$$

or

$$\Delta\lambda = \lambda_C(1 - \cos\vartheta) \tag{2.8}$$

Where $\lambda_C = \frac{h}{m_0 c}$ is the Compton wavelength.

Klein-Nishina formula

The Klein-Nishina formula gives the probability in which direction the photon gets scattered. It is more precisely the differential cross section of one photon, that gets completly elastic scattered at a free, single electron:

$$\frac{d\sigma}{d\Omega} = Z r_0 \left(\frac{1}{1 + \alpha(1 - \cos\vartheta)}\right)^2 \left(\frac{1 + \cos^2\vartheta}{2}\right) \left(1 + \frac{\alpha^2(1 - \cos^2\vartheta)}{(1 + \cos^2\vartheta)[1 + \alpha(1 - \cos\vartheta)]}\right)$$

Here is $\alpha = \frac{h\nu}{m_e c^2}$ and r_0 the classical electron radius $2,818 \cdot 10^{-15}$m. You can see the distribution in figure 2.4. It is obvious that forward scattering is preferred at high energies as we have in our experiment.

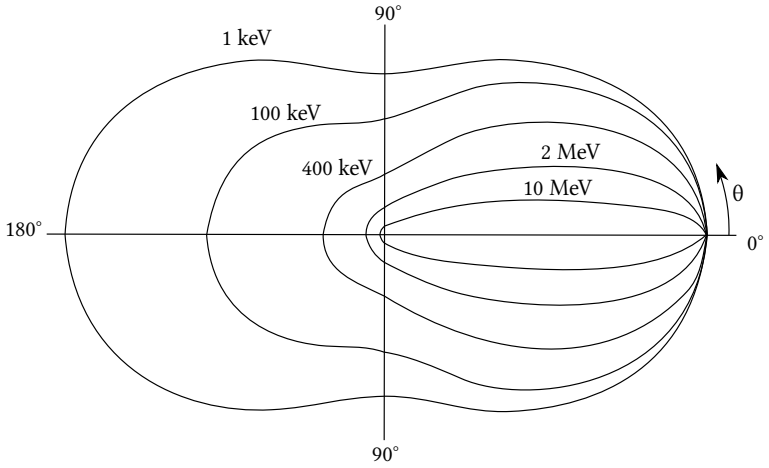

Figure 2.4: Klein-Nishina formula

2.3.4 The characteristic γ-ray spectrum

Figure 2.5 shows a typical γ-spectrum, which results of the three interactions that have been discussed previous.
The photopeak is the result of the photoelectric effect that was described in 2.3.1: It occurs when the scattered photon activates an electron in the szintillator which relaxes later by emitting another photon. It is mportant that the whole amount of energy of the incoming photon is transferred. It is the phenomena we're looking for in our evaluation.
The Compton edge is the result of equation 2.5: If the photon is scattered at an angle of 180° it transferres the maximum energy amount unto the electron:

$$E_{e,kin} = E_\gamma - E_{\gamma'} = E_\gamma - \frac{E_\gamma}{1 + \frac{E_\gamma}{m_e c^2}(1 - \cos\vartheta)} \tag{2.9}$$

with $\vartheta = 180°$:

$$E_{e,kinmax} = \frac{2E_\gamma^2}{m_e c^2 + 2E_\gamma} \tag{2.10}$$

In the spectrum you see a continuum from 0 unto the Compton edge. In our experiment the scattering takes place in the plastic szinitillator.
The escape peak is connected to the discussed pair production: If the generated electron positron pair annihilates, two photons with the energy of 511 keV will occur.

2.4 Functionality of a szintillation detector

In the experiment a szintillation detector is used for the detection of the photons. The radiation strikes the szintillator crystal, in our case NaI, which is doped with Thallium. In account of

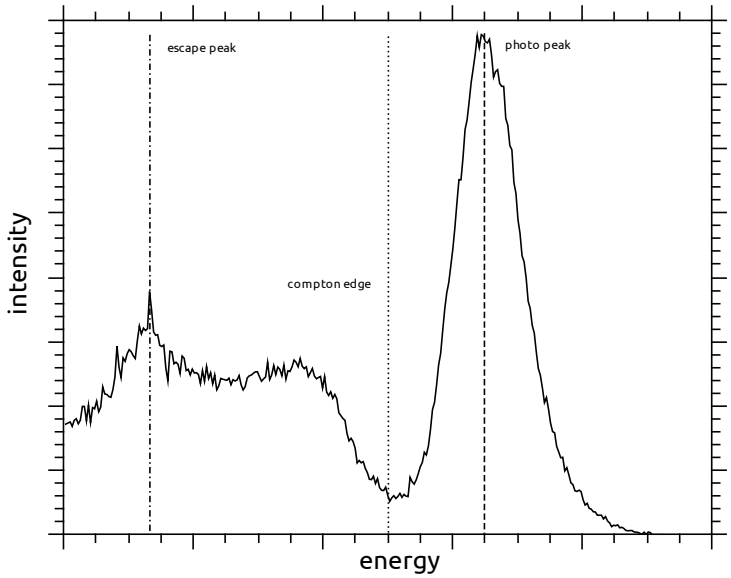

Figure 2.5: A typical γ-spectrum with photopeak, Compton edge and Escape peak

this electrons are lifted from the valence band into the conduction band, where they can freely move until they hit a defect. Now they fall down to the energy level of the defect, which is located in the valence-conduction band gap, and emitt photons of the energy between the valence band and the energy level of the defect. Therefore the photons have a wavelength within the visible window and can be detected with a common photomultiplier. The photomultiplier

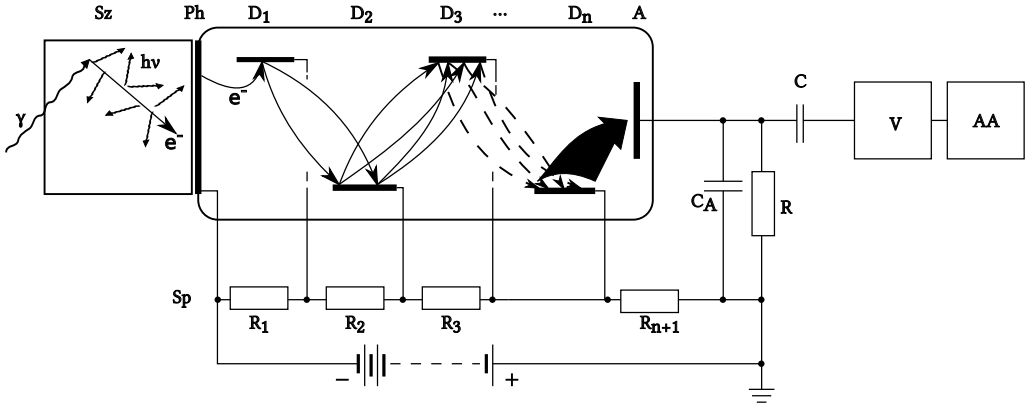

Figure 2.6: Sketch of the szintillation detector with photomultiplier

transforms the optical signal into an electrical signal: The incoming photons hit the photocathode of the photomultiplier and strike out electrons through the photoelectric effect. Now the electrons are accelerated by voltage to the first dynode, where every electron strikes out

several other electrons. These electrons are again accelerated to the next dynode, where again every electron strikes out several secondary electrons. This incident is repeated a few times until the original signal is amplified by the factor of $10^5 - 10^8$.

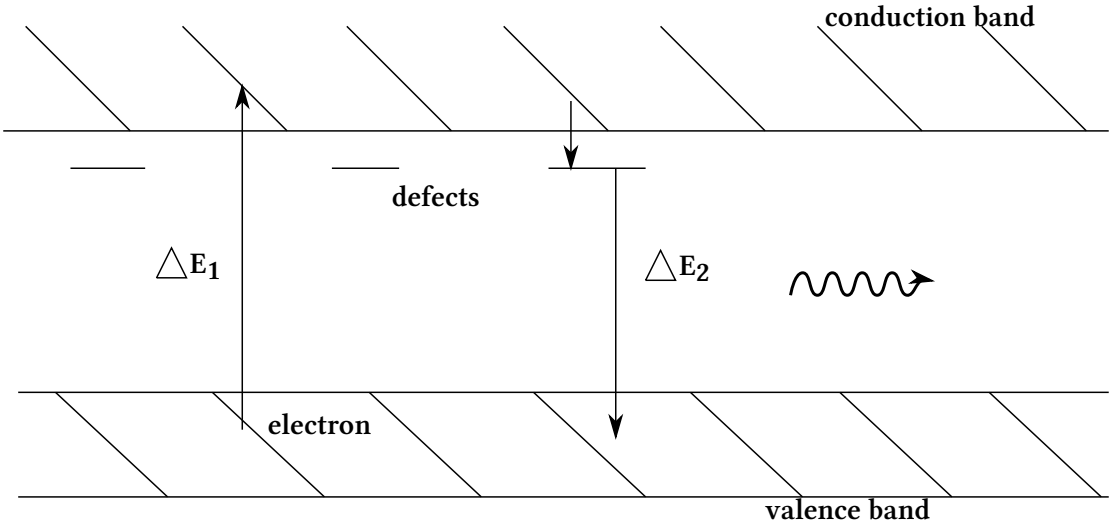

Figure 2.7: Band structure

3 Experimental setup and accomplishment

3.1 Experimental setup

The Compton scattering gets analyzed with the help of a NaI szintillator and a plastic szintillator. As γ-sources ^{137}Cs and ^{22}Na were used, in which ^{22}Na was just needed to gauge the NaI szintillator. The emitted photons strike the plastic szintillator, which has the function of an active scattering medium. The scattered photons are detected with the NaI szintillator.

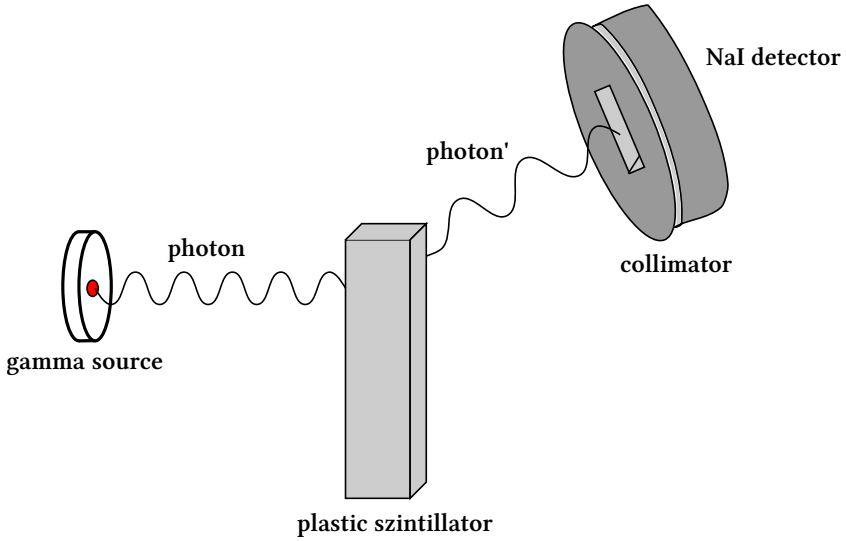

Figure 3.1: Scheme of the scattering process

This experimental setup enables us to measure the energy of the photons after the collision in dependence of the scattering angle, as well as the calculation of the energy of the electrons on which the photons were scattered, because the electrons depose their energy in the plastic szintillator. We only measure the events when both detectors produce a signal in a short time window with the help of an coincidence circuit, on which we focus in the next section. Thereby we admit to measure random events that would degrade our result. Because of the fact that the plastic detector is much faster than the NaI detector, we have to delay the signal of the plastic detector. This is realised through long cabels. The delay times are shown in figure 3.2.

3.2 Signal processing

A already said we used a coincidence circuit to dispose just the events that were detected in both detectors at almost the same time. The circuit shown in figure 3.2 consists of different electric components that make sure that the evaluation software records just true signals and no other random events. In the following e take a closer look upon some electric components:

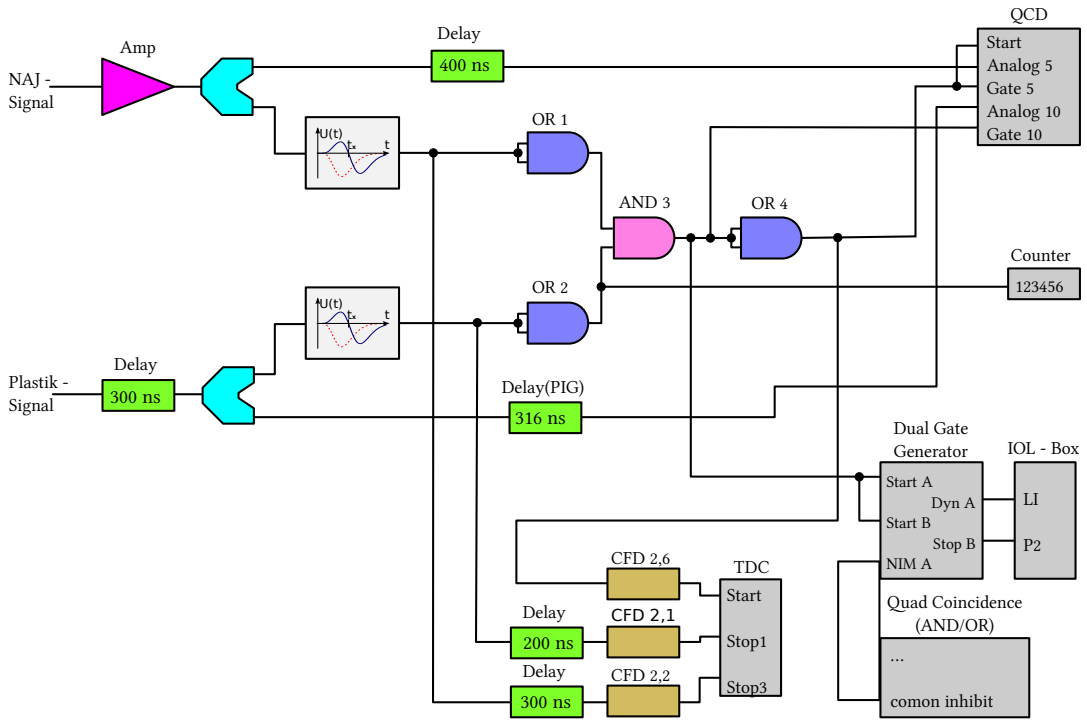

Figure 3.2: Coincidence circuit

3.2.1 Constant Fraction Discriminator (CFD)

With the help of a constant fraction discriminator a digital signal is created out of an analog signal. In general this is realized by displaying a digital signal if the analog signal oversteps a given barrier. It can be realised on different ways (see figure 3.3): The CFD is a relatively complex method, but it transformes the signal very exact. The less complex leading edge discriminator only displays a signal if the analog signal oversteps a given barrier. It is problematic that in case of signals with different amplitudes the outgoing signals are created at different times. To prevent this problem called »walk«, the CFD delays the incoming signal by a adjustable time and mute and invert it at the same. The sum of these two signals have a zero crossing, which marks the barrier.

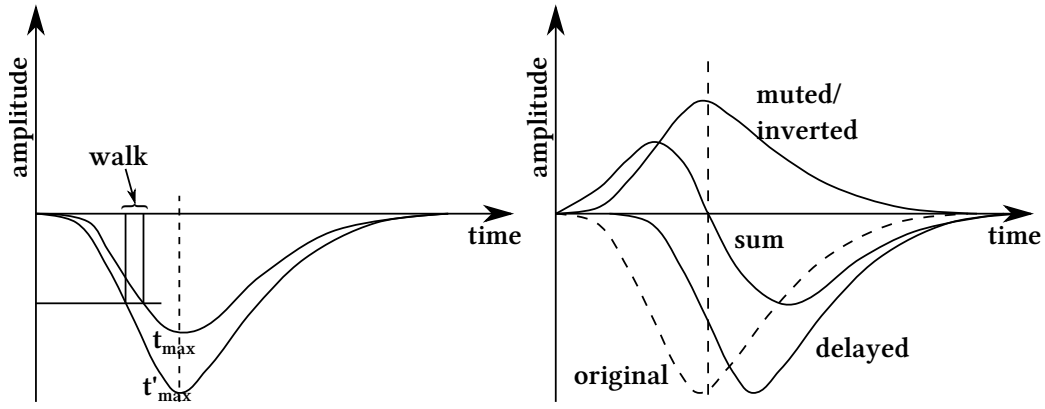

Figure 3.3: Left: Leading Edge; Right: Constant Fraction

3.2.2 AND/OR logic

The AND logic lets the signal only pass if it gets a signal from both of the two inputs. The module can also be changed to an OR logic, then it lets the signal pass if there is at least a signal at one input.

3.2.3 Time to Digital Converter (TDC)

This module transforms a period of time into a binary number. It gets started by a signal and stops by another signal. The TDC is quite important for this experiment, because it measures the delay between the plastic szintillator and the NaI szintillator.

3.2.4 Charge to digital converter (QDC)

A charge to digital converter measures the charge at the income by integrating the voltage over a given time. Subsequent the charge is displayed in a binary signal and can be processed by a PC.

3.2.5 Gate generator

The gate generator creates an outgoing signal of a constant duration for every incoming signal, independent of the length of the signal. The length of the outgoing signal can be chosen by the experimentator.

3.3 Accomplishment

In the beginning we checked the coincidence circuit for about an hour before we calibrated the NaI detector by relating the energy of characteristic points of the emitted γ-rays of the ^{137}Cs and ^{22}Na sources to the channel numbers where they appeared. This is possible, because the

relation between channel number and energy is linear.
After this we measured the photopeak of the scattered photons in the NaI detector at several angles from 40° up to 180°. Out of this peaks we were able to calculate the wavelength or rather the energy of the scattered photons.

4 Evaluation

4.1 Energy gauging

The purpose of this part of the evaluation is to create a correlation between the measured channel numbers and the photon energy. We use the photopeaks of ^{137}Cs and 22Na with known energies and the pedestal, the peak the QDC creates when there is no incoming signal, so that we have three points which we can use for a linear fit. This measurement was created without the coincidence coupling to speed the counting up but without affecting the result. With the data points aside we were able to create a linear fit to convert the measured channel into an energy.

	Channel	Energy [keV]
Cs	412,6	662
Na	352,6	511
Pedestal	108,6	0

Table 4.1: Data for the linear gauging fit

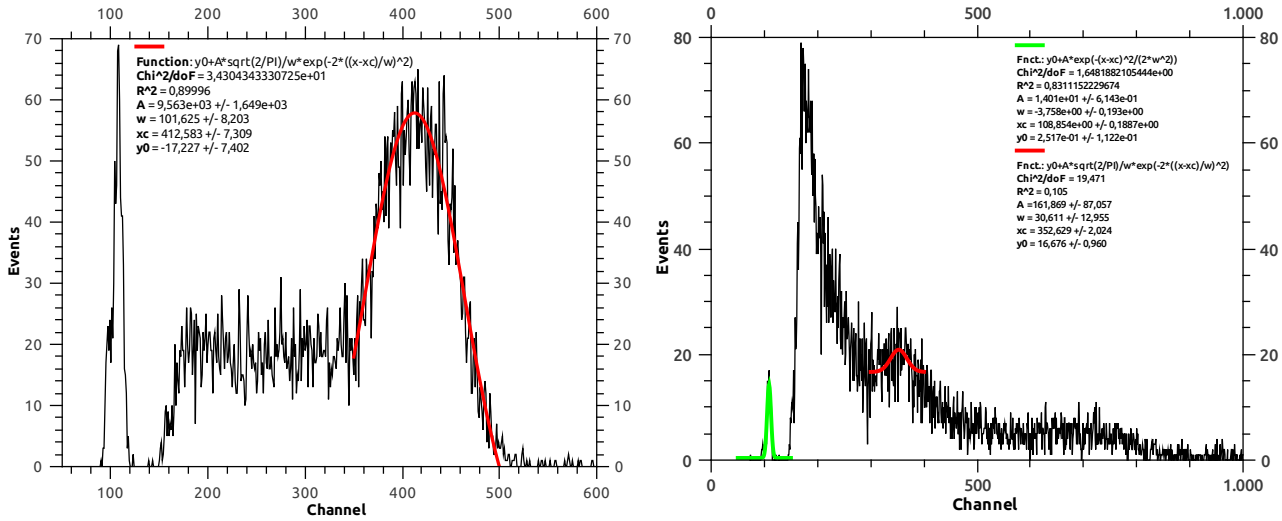

(a) Caesium gauging fit

(b) Sodium gauging fit

Figure 4.1: Fits of the gauging measurements for caesium and sodium

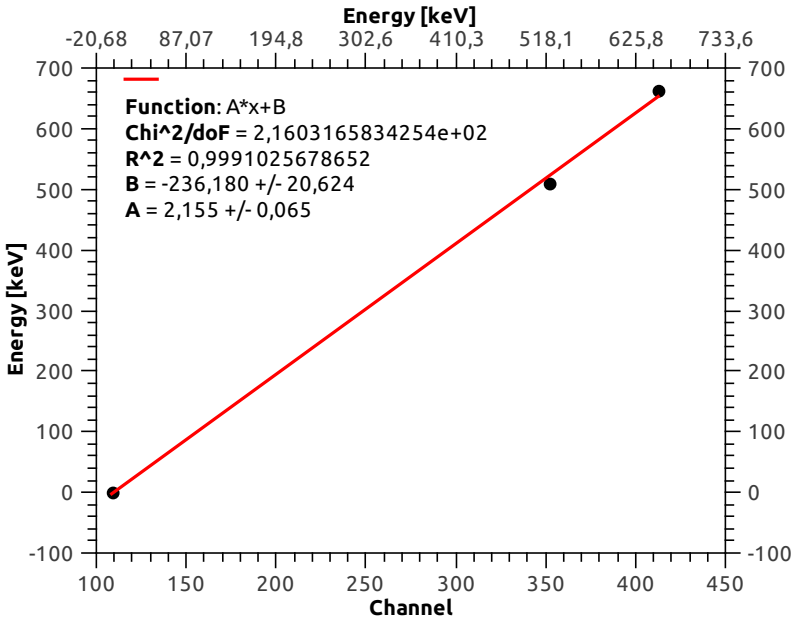

Figure 4.2: Linear gauging fit

As you can see, the formula we get is $y = (2,155 \pm 0,065) \cdot x - (236,18 \pm 20,624)$, where y corresponds to the energy in keV and x corresponds to the channel number. [4.1]

4.2 Backscattering

In this part we want to determine the value of the Compton wavelength of an electron. Therefor we measure the energy of the backscattered photons, which have by formula 2.5 at an angle of 180° a wavelength of

$$\lambda_{Compton} = \frac{1}{2}\left(\frac{hc}{E'} - \frac{hc}{E}\right)$$

E is caesium's known photopeak energy of 662 keV and E' was determined by the fit aside. We find E' at channel 198,113 ± 0,505 or an energy of (190,753 ± 1,088) keV. With this we find the Compton wavelength $\lambda_{Compton}$ as $\lambda_{Compton} = (2,323 \pm 0,019) \cdot 10^{-12}$m. The literature value is $2,426 \cdot$

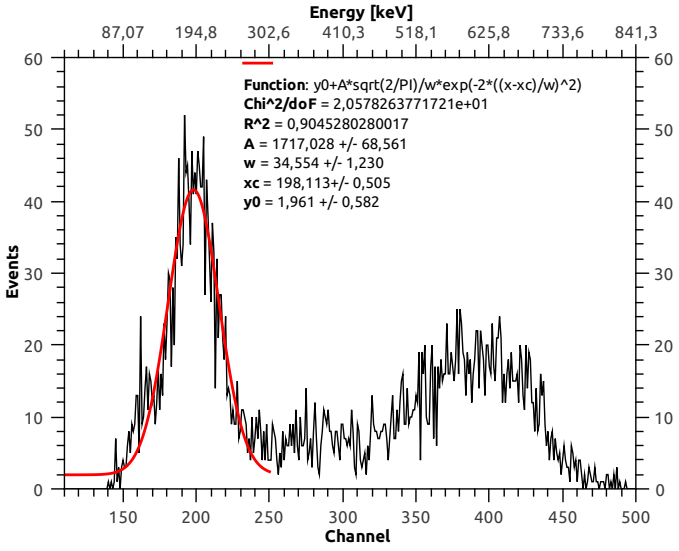

Figure 4.3: Backscattering fit

10^{-12}m. So our measured value varies with an error of 5% around the literature value, which is quite a good result, even not as good as expected.

4.3 Compton scattering as a function of the scattering angle

For the following parts we need the energy of the scattered photons for the angles 40°, 60°, 80°, 100°, 120°, 140°, 160° and 180°. We get them by fitting with a Gaussian distribution.

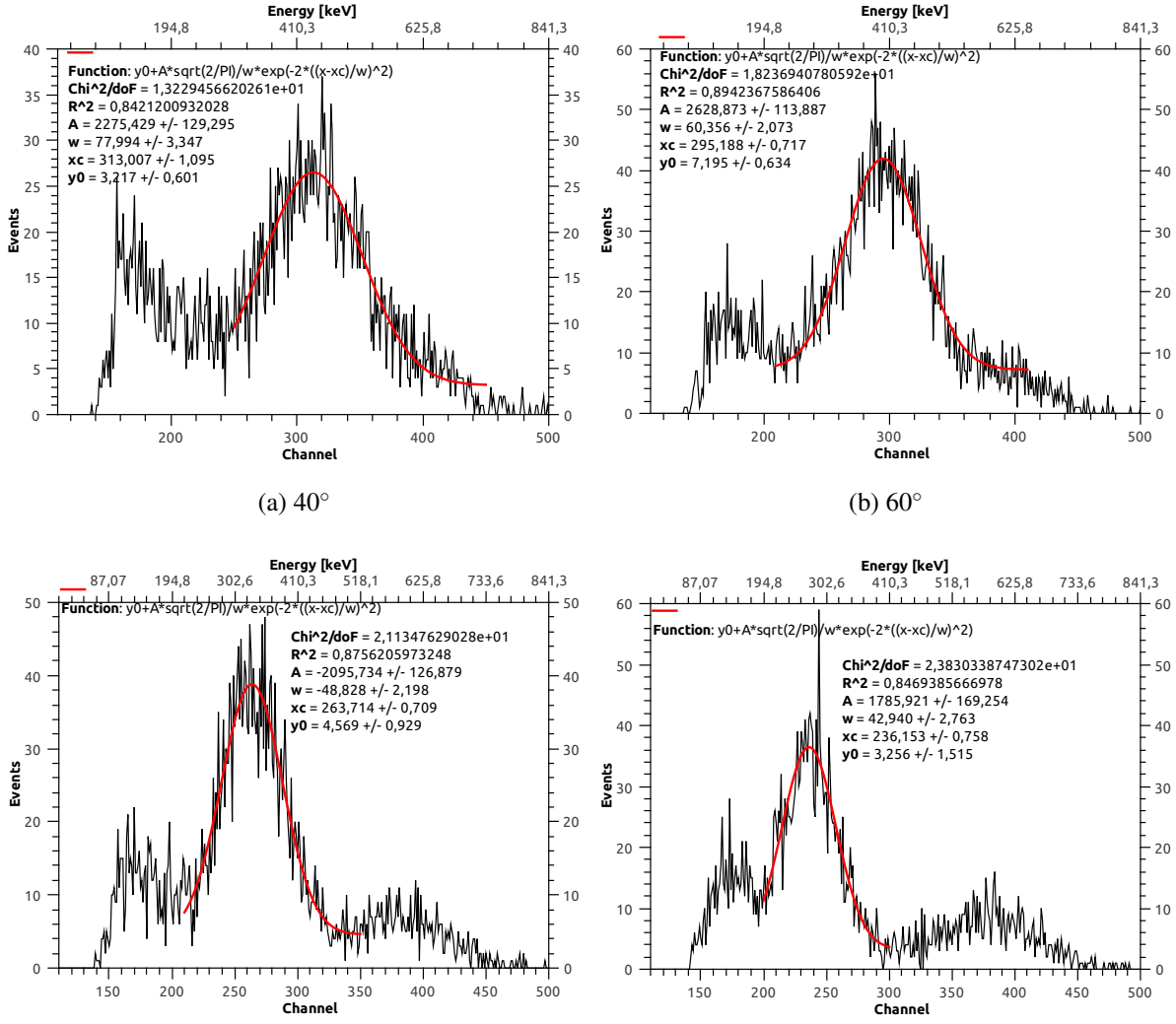

(a) 40°

(b) 60°

(c) 80°

(d) 100°

Figure 4.4: Energy distribution at 40° to 100°

From the fits we get the following data 4.2, which we need for further analysis. The energy is

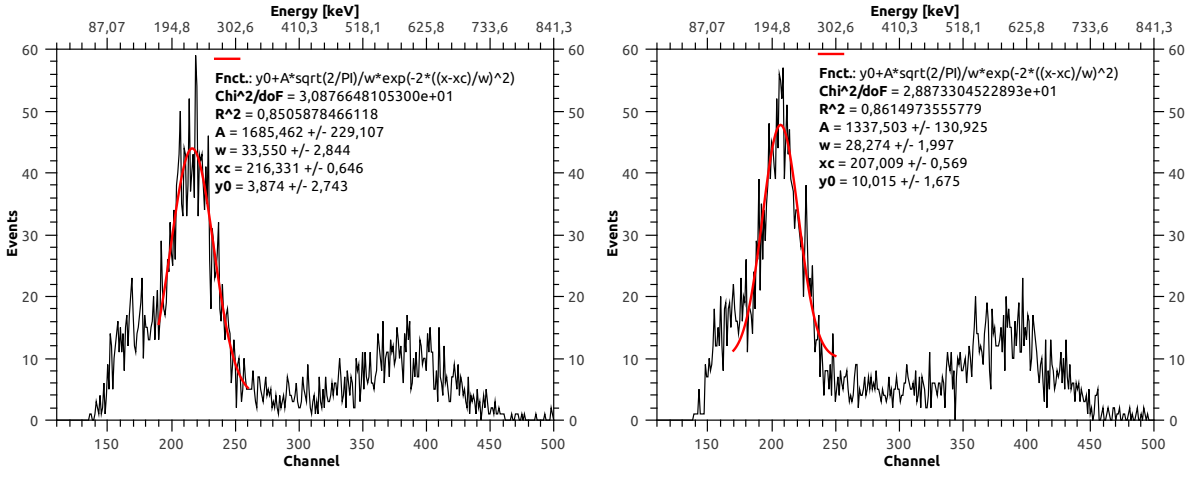

(a) 120°

(b) 140°

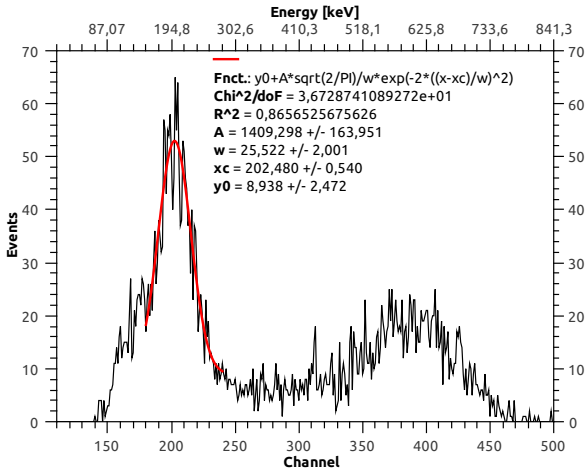

(c) 160°

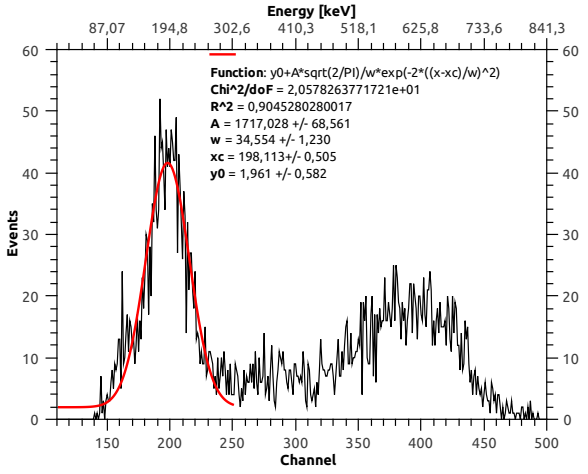

(d) 180°

Figure 4.5: Energy distribution at 120° to 180°

given by the channel number xc, which can be converted into an energy with formula 4.1. $\Delta\frac{1}{E}$ is given by $\Delta\frac{1}{E} = \frac{1}{E'} - \frac{1}{E}$.

angle	40°	60°	80°	100°	120°	140°	160°	180°
energy [keV]	438,35	399,95	332,12	272,73	230,01	209,92	200,16	190,75
$\Delta\frac{1}{E}$ $[\frac{1}{keV}]$	0,771	0,990	1,500	2,156	2,837	3,25	3,485	3,732

Table 4.2: Data for the different angles

4.3.1 Connection between the scattered photon energy and the scattering angle

We can now plot the scattered photon energy against the scattering angle and compare it with formula 2.5.

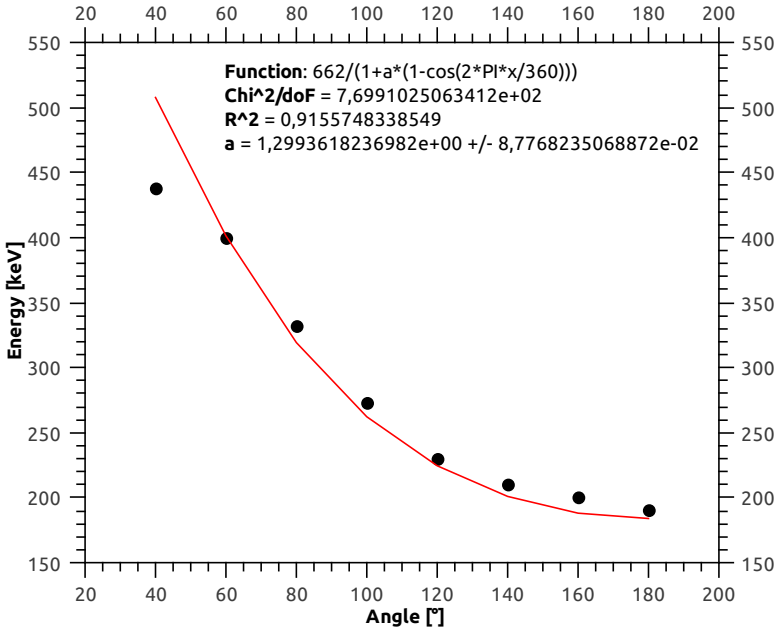

Figure 4.6: Plot of the scattered photon energy against the scattering angle

As we can see, the measured data fits quite well with the theory. The fit parameter a has a value of $1,2993 \pm 0,0878$, whereas the theoretical value would be 1,2955.

4.3.2 Plot of $\Delta\frac{1}{E}$ against $1 - cos\theta$

In this part we want to analyse the connection between $\Delta\frac{1}{E}$ and $1 - cos\theta$, which should in accordance with formula 2.6 be linear.

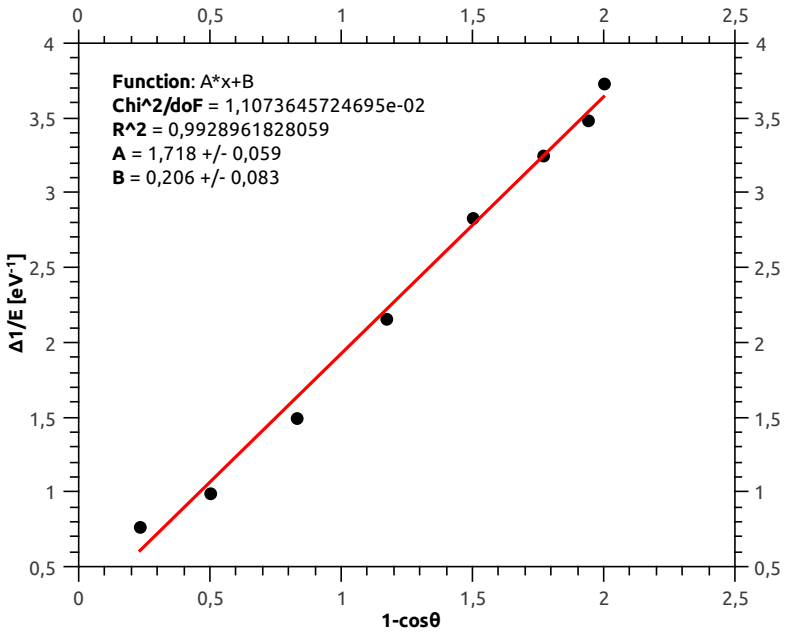

Figure 4.7: Plot of $\Delta\frac{1}{E}$ against $1-cos\theta$

As we can see, the correlation between the measured data and the fitted line is very good. We can now calculate the electron mass using the draft of the fitted plot. Referring to formula 2.6 $\Delta\frac{1}{E}$ is proportional to $\frac{1-cos\theta}{m_0c^2}$. If we take the inverse of the draft, we get the electron mass:

$$m_e = \frac{1}{1,718 \pm 0,059} \approx 0,582 \pm 0,021 \hat{=} (582 \pm 21)\,\text{keV}.$$

The theoretical value of the energy mass is 511 keV, so we miss the literature value with an error of about 12%.

4.3.3 Cross section

angle [°]	40	60	80	100	120	140	160	180
const	26,495	41,948	38,815	36,497	43,958	47,759	52,996	47,609
ω	77,984	60,356	48,828	42,940	33,550	28,274	25,522	34,554
N	524388	470996	505666	521161	492443	477645	477602	377688
$\frac{const \cdot \omega}{N}[10^{-3}]$	3,941	5,375	3,748	3,007	2,995	2,827	2,832	3,807

Table 4.3: Data for measuring the cross section

In the end we want to see if the calculated cross section fits the theoretical values. The theoretical cross section, as given in formula 2.9, should be proportional to $\frac{const \cdot \omega}{N}$, whereas ω is given by the fits, *const* is the heigth of the Gaussian distribution, which can be calculated as the difference between the value of the Gaussian distribution at xc and the offset y0 and N is the number of total events that occured. Now we can plot the data against the angle. If we compare it with the theoretical Klein-Nishina-formula, we see that all except the points for 60° and 180° fit quite well. For better results the measurment time had has to been increased, so that more statistical data could have been raised.

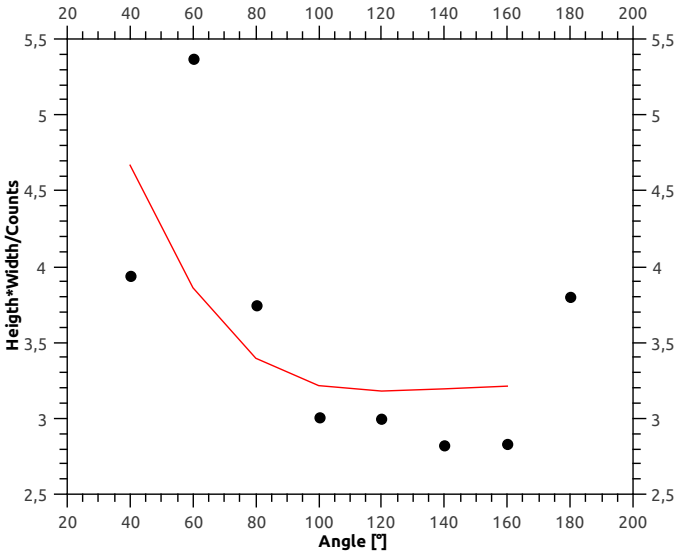

Figure 4.8: Comparison between measured and calculated cross section

4.4 Energy gauging after the measurement

After we took all our measurements, we gathered a second gauging measurement with caesium to see, if the correlation between the channel number and the energy was still unchanged. Changes can happen because of changes for example in the room temperature, which is not very unlikely, if you work for a few hours in a closed room. In the beginning of our mea-

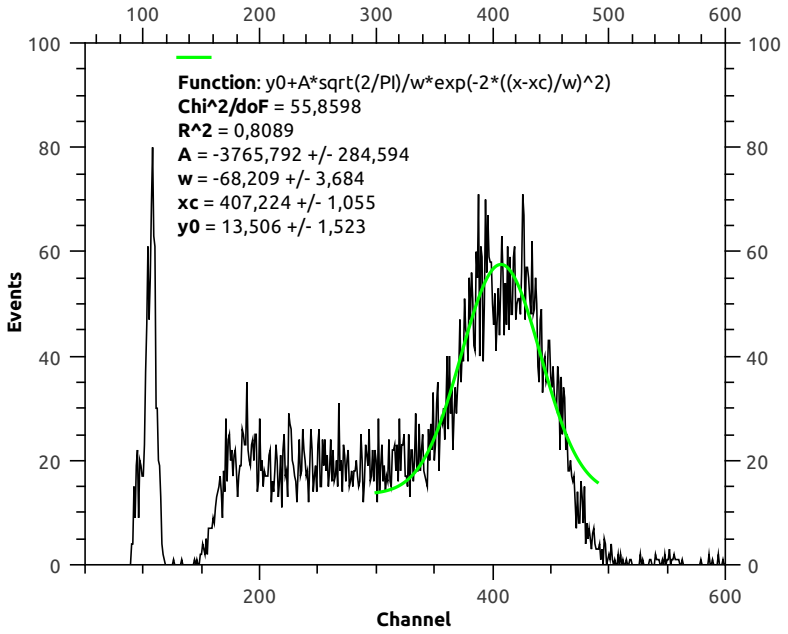

Figure 4.9: Second gauging fit

surement the caesium peak was at channel $412 \pm 7,309$, after the measurement at channel $407 \pm 1,055$. So we see that the calibration we made in the beginning is still valid for the afterwards taken measurements.

Bibliography

[1] D. Meschede: *Gerthsen Physik*, 23., überarbeitete Auflauge erschienen im Springer-Verlag

[2] Ingolf V. Hertel, Claus-Peter Schulz: *Atome, Moleküle und optische Physik 1 - Atomphysik und Grundlagen der Spektroskopie* erschienen im Springer-Verlag

[3] Bogdan Povh, Klaus Rith, Christoph Scholz, Frank Zetsche: *Teilchen und Kerne - Eine Einführung in die physikalischen Konzepte*, 8. Auflage erschienen im Springer-Verlag

[4] Demtröder: *Experimentalphysik 4*, 3. Auflage, erschienen im Springer-Verlag

[5] H. Haken, H. C. Wolf: *Atom- und Quantenphysik*, 7. Auflage, erschienen im Springer-Verlag

List of Tables

List of Figures